


RESEARCH ARTICLE

Open Access



Microglia Sirt6 modulates the transcriptional activity of NRF2 to ameliorate high-fat diet-induced obesity

Xiaoxia Xiao¹, Huiling Hu^{2,3}, Yadi Zhong¹, Yingjian Chen¹, Kaijia Tang¹, Zhisen Pan⁴, Jiawen Huang¹, Xiaoying Yang^{5*}, Qi Wang^{1*} and Yong Gao^{1*} 

Abstract

Background Microglia play a pivotal role in neuroinflammation, while obesity triggers hypothalamic microglia activation and inflammation. Sirt6 is an important regulator of energy metabolism in many peripheral tissues and hypothalamic anorexic neurons. However, the exact mechanism for microglia Sirt6 in controlling high-fat diet-induced obesity remain unknown.

Methods Microglia Sirt6 expression levels under various nutritional conditions were measured in the hypothalamus of mice. Also, microglia Sirt6-deficient mice were provided various diets to monitor metabolic changes and hypothalamic inflammatory response. Besides, RNA-seq and Co-IP of microglia with Sirt6 alterations were conducted to further investigate the detailed mechanism by which Sirt6 modulated microglia activity.

Results We found that Sirt6 was downregulated in hypothalamic microglia in mice given a high-fat diet (HFD). Additionally, knockout of microglia Sirt6 exacerbated high-fat diet-induced hypothalamic microglial activation and inflammation. As a result, mice were more prone to obesity, exhibiting a decrease in energy expenditure, impaired glucose tolerance, insulin and leptin resistance, and increased food intake. In vitro, Sirt6 overexpression in BV2 cells displayed protective effects against oleic acid and palmitic acid treatment-derived inflammatory response. Mechanically, Sirt6 deacetylated and stabilised NRF2 to increase the expression of anti-oxidative genes and defend against reactive oxygen species overload. Pharmacological inhibition of NRF2 eliminated the beneficial modulating effects of Sirt6 on microglial activity.

Conclusion Collectively, our results revealed that microglial Sirt6 was a primary contributor of microglial activation in the central regulation of obesity. Thus, microglial Sirt6 may be an important therapeutic target for obesity.

Keywords Sirt6, Microglial activation, Hypothalamic inflammation, NRF2, Obesity

*Correspondence:

Xiaoying Yang

yxyxiaoliqq@163.com

Qi Wang

wangqi@gzucm.edu.cn

Yong Gao

gaoyong@gzucm.edu.cn

¹Science and Technology Innovation Center, Guangzhou University of Chinese Medicine, Guangzhou 510006, China

²Department of Clinical Laboratory, Sun Yat-Sen Memorial Hospital, Sun Yat-Sen University, Guangzhou 510289, China

³Guangdong Provincial Key Laboratory of Malignant Tumor Epigenetics and Gene Regulation, Sun Yat-Sen Memorial Hospital, Sun Yat-Sen University, Guangzhou 510289, China

⁴First Affiliated Hospital, Guangzhou University of Chinese Medicine, Guangzhou 510006, China

⁵Jiangsu Key Laboratory of Immunity and Metabolism, Department of Pathogen Biology and Immunology, Xuzhou Medical University, Xuzhou 221004, Jiangsu, China



© The Author(s) 2023. **Open Access** This article is licensed under a Creative Commons Attribution 4.0 International License, which permits use, sharing, adaptation, distribution and reproduction in any medium or format, as long as you give appropriate credit to the original author(s) and the source, provide a link to the Creative Commons licence, and indicate if changes were made. The images or other third party material in this article are included in the article's Creative Commons licence, unless indicated otherwise in a credit line to the material. If material is not included in the article's Creative Commons licence and your intended use is not permitted by statutory regulation or exceeds the permitted use, you will need to obtain permission directly from the copyright holder. To view a copy of this licence, visit <http://creativecommons.org/licenses/by/4.0/>.

Introduction

Achieving an energy balance in the body involves numerous biochemical reactions and hormonal signalling pathways. However, a persistent positive energy balance leads to common metabolic-related diseases such as obesity (Nadal et al. 2017). The hypothalamus is involved in the regulation of energy metabolism. Additionally, specific areas of the hypothalamus, such as the paraventricular nucleus (PVN), perifornical area (PFA), lateral hypothalamic area (LHA), and arcuate nucleus (ARC), synergistically regulate energy metabolism by integrating neural, nutritional, and hormonal signals (Schwartz et al. 2000). Microglia are the immune-competent cells of the brain and their activation may result in abnormal neurons in the hypothalamus, causing glucose and lipid metabolism disorders in the body. The mechanism of this process involves activated hypothalamic microglia producing a variety of pro-inflammatory cytokines that influence metabolism by inducing changes in neuronal activity (Reis et al. 2015; Valdearcos et al. 2014). HFD exposure triggers microglial activation and hypothalamic inflammation, which is manifested by altered microglial morphology (transformed to an M1-like pro-inflammatory phenotype), activation of inflammatory signalling, and increased expression of inflammatory cytokines (Mendes et al. 2018; André et al. 2017). Furthermore, hypothalamic inflammation occurs before significant weight gain (Thaler et al. 2012), suggesting that it may be an upstream event in diet-induced obesity (DIO). Drug depletion of microglia limits diet-induced weight gain. Conversely, specific activation of microglia induces food intake and subsequent weight gain in mice (Valdearcos et al. 2017). These findings support the potential of microglia as central energy regulators. However, the extent to which inflammatory activation of microglia affects metabolism is uncertain, and further investigation into the role of microglia in coordinating metabolism is necessary.

Sirtuin 6 (Sirt6) is a member of the Sirtuin family of NAD⁺-dependent enzymes, with three forms of enzymatic activity: deacetylase, adenosine diphosphotransferase, and defat acylase. As a chromatin-associated nuclear protein, Sirt6 is highly expressed in the central nervous system (CNS) and it reduces inflammatory damage caused by microglial activation. For instance, endothelial Sirt6 plays a protective role in cerebral ischemia/reperfusion injury (Liberale et al. 2020). Additionally, the pharmacological activation of Sirt6 ameliorates neuroinflammation and attenuates brain injury in mice with ischemic stroke (He et al. 2021). As an NAD⁺-dependent enzyme, one primary function of Sirt6 is to regulate energy metabolism in the body. Initial studies found that Sirt6-deficient mice exhibited severe metabolic defects (Mostoslavsky et al. 2006). Subsequent studies established that Sirt6 transgenic mice were resistant to

high-fat diet-induced obesity, manifested by less fat accumulation (Kanfi et al. 2010). Similarly, adipose-specific Sirt6 knockout mice and myeloid-specific Sirt6 knockout mice are more susceptible to DIO (Yao et al. 2017; Lee et al. 2017). Recent studies have shown that Sirt6 may regulate metabolism in relation to its anti-inflammatory effect. Fat-specific Sirt6 deficiency promotes adipose tissue inflammatory response, which contributes to insulin resistance (Kuang et al. 2017). Also, myeloid-specific Sirt6 deletion promotes M1-type pro-inflammatory macrophage expression in mice. As a result, mice exhibit increased hepatic tissue inflammation and aggravated hepatic steatosis (Lee et al. 2017). Currently, the role of Sirt6 in diet-induced obesity-related hypothalamic inflammation has not been reported. The mechanism by which microglia Sirt6 coordinates DIO also remains to be explored.

Transcription factor NRF2 (Nuclear Factor Erythroid 2-related Factor 2) is one of the main regulators of the antioxidant defence system in the body. Normally, NRF2 associates with Kelch-like ECH-associated Protein 1 (Keap1) in the cytoplasm and is degraded by the ubiquitinase Cullin3. During oxidative stress, NRF2 dissociates from the complex and translocates to the nucleus, where it binds to DNA at the antioxidant response elements (ARE) position, thereby promoting the expression of downstream antioxidant enzymes (Silva-Islas and Maldonado 2018). Activation of NRF2 is associated with the amelioration of oxidative stress and reduction of neuroinflammatory responses. In neurodegenerative diseases associated with oxidative homeostasis, such as Parkinson's disease, promoting the NRF2 antioxidant pathway improves mitochondrial and neuronal function and protects the dopaminergic neurons of mice from oxidative damage (Martín-Montañez et al. 2021). Besides, NRF2 deficiency exacerbates gliosis and neuroinflammatory responses in mouse models with combined tauopathy and amyloidopathy (Rojo et al. 2018). Additionally, enhancing the p21-NRF2 axis of microglia ameliorates neurodegeneration by suppressing neuroinflammation (Nakano-Kobayashi et al. 2020). The potential of NRF2 in metabolic regulation has gradually emerged in recent years. NRF2 has been reported to prevent oxidative stress and restore insulin secretion in mouse pancreatic β -cells in the context of reactive species damage (Yagishita et al. 2014). NRF2 also improves insulin and leptin resistance in mice by reducing oxidative damage in the mouse hypothalamus (Yagishita et al. 2017). These findings highlight the role of NRF2 in the CNS and metabolic-related diseases. However, the exact role of NRF2 and its upstream and downstream effectors in metabolic regulation still requires further investigation.

The results from our study reveal that Sirt6 is involved in the regulation of M1/M2 phenotypic transition

in microglia, and further confirm that hypothalamic microglia Sirt6 plays a critical role in long-term high-fat diet-induced obesity. Furthermore, we found that Sirt6 maintains its stability by deacetylating NRF2, thereby achieving the purpose of anti-inflammation and anti-oxidation and ultimately regulating the damage caused by a HFD.

Materials and methods

Animal and experimental designs

Male C57BL/6J mice (6–8 weeks old) were provided by the Animal Experiment Centre of Guangzhou University of Chinese Medicine and Cx3cr1-Cre mice were purchased from Cyagen. Additionally, SIRT6^{fllox/fllox} mice (hereafter referred to as SIRT6^{fl/fl}) that were originally purchased from the Jackson Laboratory (Bar Harbor, ME, USA) were donated by the West China Hospital of Sichuan University (Zhang et al. 2021). Microglia Sirt6 conditional knockout mice (hereafter referred to as SIRT6^{Mic-/-}) were produced by mating SIRT6^{fl/fl} mice with Cx3cr1-Cre mice. All animals were housed under standard laboratory conditions with a 12-h light/dark cycle. Mice were allowed access to a standard chow diet (SD) or HFD (research diet, D12492, USA) for 12 weeks. Besides, all animals had free access to food and water throughout the experiment unless otherwise stated. All animal handling complied with the guidelines of the Animal Ethics Committee of Guangzhou University of Chinese Medicine, and the experimental protocols were approved.

At the end of the study, the mice were anesthetized by Pentobarbital sodium salt (57-33-0, sigma). Next, the mice were euthanized by cardiac perfusion or cervical dislocation. Part of the tissue was fixed in 4% paraformaldehyde solution and part was kept in a freezer at -80 °C. The collected blood was centrifuged to obtain serum, which was also stored at -80 °C. The number of animals used is detailed in the figure legends.

Haematoxylin and eosin (HE) staining

Liver and adipose tissue samples were fixed with 4% paraformaldehyde, dehydrated using different concentration gradients of ethanol, embedded in paraffin, and cut into 4 µm thick sections. Sections were deparaffinised, stained with haematoxylin and eosin (HE), dehydrated, and mounted with neutral gum. The staining of the tissue sections was imaged under a Nikon microscope (Eclipse, 80i).

Oil red O staining

Liver tissue was fixed with 4% paraformaldehyde, dehydrated with 30% sucrose solution, embedded in OCT gel, and cut into 7 µm thick sections using a Leica CM1950 frozen microtome. Sections were stained with oil red,

differentiated with 60% isopropanol, further stained with haematoxylin, and then finally mounted. Images were collected using a Nikon microscope.

Fat assay of mice

Mice after 12 weeks of the HFD were subjected to micro-CT scanning. Subsequently, the brown fat, subcutaneous fat, and epididymal fat of the mice were analyzed and reconstructed using the software.

Serum biochemical test

Serum insulin was measured using a mouse insulin (INS) ELISA kit (RX202485M, Ruixin Biotech) and calculated according to the directions. Serum norepinephrine was determined with a mouse norepinephrine ELISA Kit and calculated according to the manufacturer's instructions.

Glucose tolerance test (GTT), insulin tolerance test (ITT), and pyruvate tolerance test (PTT)

Following our previously reported methods (Sun et al. 2021), mice were subjected to GTT, ITT and PTT tests after 12 weeks of the HFD. Briefly, for GTT, after fasting for 16 h, mice were injected intraperitoneally with glucose (1.5 g/kg) and the tail vein blood glucose was measured at six time points (0, 15, 30, 60, 90, 120 min) with a blood glucose meter. As for ITT, mice were injected intraperitoneally with human insulin (0.75 U/kg) after fasting for 4 h, and the tail vein blood glucose was measured at the same time points as for GTT. Regarding PTT, mice were injected intraperitoneally with sodium pyruvate (1 g/kg) after fasting for 16 h, and the tail vein blood glucose was measured at the same time points as the other two tests.

Leptin function and sensitivity studies

Murine Leptin (AF-450-31-1MG, PeproTech) was intraperitoneally injected into SIRT6^{fl/fl} and SIRT6^{Mic-/-} mice. Next, the food intake and body weight of the mice were measured. Additionally, SIRT6^{fl/fl} and SIRT6^{Mic-/-} mice were perfused 45 min after leptin injection and the expression of P-STAT3 (Ser727) in mouse brain tissue was detected through immunofluorescence.

Immunohistochemistry

Brown adipose tissue sections were obtained in the same manner as for HE staining, as described above. The sections were deparaffinised and rehydrated with xylene and different concentrations of ethanol. Next, 3% hydrogen peroxide was used to quench endogenous peroxidase and antigen retrieval was performed in citrate buffer. After blocking with 10% goat serum, the primary antibody UCP1 (P25874, CUSABIO) was added, the mixture was kept overnight at 4 °C, and then it was incubated with HRP-conjugated secondary antibody for 30 min at room

temperature. After DAB working solution staining and haematoxylin counterstaining, the samples were further dehydrated with increasing concentrations of ethanol and finally mounted. Image information was collected under the microscope.

Cold exposure test

Following our previous method (Tang et al. 2020), mice after 12 weeks of the HFD were transferred from room temperature to 4 °C refrigerator (BIOBASE, BYC-1000) and their body temperatures were measured at 0 h, 2 h, 4 h, and 6 h.

Metabolic parameter measurements

Mice after 12 weeks of the HFD were acclimated for 48 h in advance and energy expenditure was measured using a comprehensive laboratory animal monitoring system (CLAMS). During the experiment, the surrounding environment was kept quiet and the mice were provided sufficient water and food.

Isolation and culture of mouse primary microglia

Mice after 24 weeks of the HFD were used to isolate primary microglia. The mice were sacrificed by cervical dislocation, and their brain tissue was isolated and placed in PBS solution. The tissue masses were adopted for preparing cell suspension through mechanical grinding of Dounce homogenizer, and then the cell suspension was filtrated by a 70 µm (200 mesh) cell strainer for debris removal. After 7 min of 300 g centrifugation at a low speed, the supernatant was discarded, and the cells were collected. Percoll (17-0891-09, GE Healthcare) was mixed in 10×PBS to make solutions at three different concentrations, i.e., 30%, 37% and 70%. The collected cells were transferred to 37% Percoll solution. In a 15 ml centrifuge tube, 4 ml of 70% Percoll solution, 4 ml of 37% Percoll solution containing cells, and 4 ml of 30% Percoll solution were added in sequence, and at last, 2 ml of PBS was added. The mixture underwent 40 min of 300 g centrifugation at 18 °C. After the centrifugation, the cells were collected from the 37% and 70% gradient interfaces and washed twice with 6 ml PBS. At last, the cells were collected for Quantitative Real-Time PCR.

For the one-day-old neonatal mice, the brain of mice was collected using microsurgical forceps. The tissue was digested with trypsin (C0207, Beyotime), centrifuged, resuspended in complete medium and filtered through a 70 µm cell strainer to obtain mixed glial cells. The cells were cultured in an incubator and the medium was changed every 3 days. After 15 days of culture, the cells appeared stratified. Microglia attach to the surface of astrocytes. Next, the microglia were shaken down using a shaker, with operating conditions of 37 °C and 200 rpm, for 2 h. The collected microglia were resuspended in

complete medium to continue culturing in the incubator. At last, the cells were collected for Western blot analysis.

BV2 cells culture

BV2 cells (Wuhan University Cell Bank, China) were cultured in DMEM medium containing 10% foetal bovine serum at standard cell culture conditions (5% CO₂, 95% air). The cells were operated for no more than 10 generations.

BV2 cells treatment

Oleic acid (OA) may stimulate the formation of lipid droplets through activating FFAR4, a long-chain fatty acid receptor (Rohwedder et al. 2014; Chausse et al. 2019), while palmitic acid (PA) is a major contributor to diet-induced neuroinflammation (Chausse et al. 2019; Valdearcos et al. 2015). Here, we utilized OA&PA combination to treat the cells, thus simulating the effects of a high-fat diet stimulation. In the overexpression experiment, adenoviruses Ad-Sirt6 (Obio Technology, Shanghai, China) and Ad-GFP were used for 12 h infection of BV2 cells, and in the knockdown experiment, adenoviruses Ad-shSirt6 (Obio Technology, Shanghai, China) and Ad-shGFP were adopted for 12 h infection of BV2 cells. Subsequently, BV2 cells were cultured for 24 h in a fresh medium containing OA and PA, and to inhibit NRF2, BV2 cells were treated with ML-385 (846557-71-9, Selleck) for 12 h. At last, the cells were collected for further analysis.

Cytokine measurement

The expression levels of tumour necrosis factor alpha (TNF-α), interleukin 6 (IL-6), and interleukin 1β (IL-1β) in the culture supernatant were measured using the mouse TNF-α ELISA kit (JL10484, Jianglai, Shanghai, China), mouse IL-6 ELISA kit (JL20268, Jianglai, Shanghai, China), and mouse IL-1β ELISA kit (JL18442, Jianglai, Shanghai, China), respectively.

Co-immunoprecipitation (Co-IP) assay

Adenoviruses Ad-Sirt6 and Ad-GFP were transfected into BV2 cells, then the cells were collected to extract proteins. Experiments were performed using protein A+G agarose (Fast Flow, P2012, Beyotime). Specifically, protein A+G agarose and normal IgG of the same species as the IgG used for immunoprecipitation were added to remove non-specific binding of the protein sample. After the samples were incubated overnight with Sirt6 (67510-1-Ig, Proteintech) or NRF2 (16396-1-AP, Proteintech), protein A+G agarose was added. The mixture was shaken slowly at 4 °C for 3 h and then centrifuged and denatured. Subsequent western blot experiments were performed using Sirt6 (13572-1-AP, Proteintech) and NRF2 (ab89443, Abcam) antibodies.

For the acetylation assays, the cells were lysed in lysis buffer containing a protease inhibitor, phosphatase inhibitors, and acetylase inhibitor. Protein A+G agarose and IgG were added to remove non-specific binding of the protein sample. After the samples were incubated overnight with NRF2 (ab89443, Abcam), protein A+G agarose was added. Next, the mixture was shaken slowly at 4 °C for 3 h, then it was centrifuged and denatured. Subsequent western blot experiments were performed using Pan Acetyl-Lysine Rabbit pAb (A2391, ABclonal) to detect the acetylation levels of NRF2.

Intracellular reactive oxygen species (ROS) assay

After the preparation of the cell samples, a fluorescent probe DHE (38483-26-0, KeyGEN BioTECH) was used for ROS determination. For this process, 10 μM DHE was added to the cells, which were then incubated at 37 °C for 20 min in the dark and washed with PBS. Finally, fluorescence images were taken with a LEICA DMi8 fluorescent inverted microscope.

Immunofluorescence

Brain tissue was fixed with 4% paraformaldehyde for 48 h, dehydrated with 30% sucrose solution, and then embedded in OCT gel. The tissue was cut into 30 μm thick coronal sections with a Leica CM1950 frozen microtome. Sections were then treated with 1% Triton™ X-100 (T8787, Sigma-Aldrich) and 5% BSA (A8020, Solarbio) for 1 h at room temperature and subsequently incubated overnight at 4 °C with the following primary antibodies: Anti-Iba1 antibody (ab5076, Abcam), Sirt6 (13572-1-AP, Proteintech), TNF-α (A11534, ABclonal), and P-STAT3 (11,046, SAB). Donkey Anti-Rabbit IgG H&L (Alexa Fluor® 488, ab150073, Abcam) was used for single staining, while Donkey Anti-Rabbit IgG H&L and Donkey Anti-Goat IgG H&L (Alexa Fluor® 594, ab150132, Abcam) were employed for double staining. After the antibody was incubated for 1 h at room temperature, the

slides were mounted with DAPI-containing mounting medium (S2110, Solarbio). Finally, fluorescence images were acquired using an SP8 Leica confocal fluorescence microscope (TCS-SP8).

For cellular immunofluorescence, cell samples were fixed with 4% paraformaldehyde for 20 min at room temperature, treated with 0.3% Triton™ X-100 for 15 min, and blocked with 5% BSA for 1 h. The main primary antibodies used were: CD68 (BA3638, Boster), TNF-α (A11534, ABclonal), and NRF2 (16396-1-AP, Proteintech). Besides, Alexa Fluor 594-conjugated AffiniPure Goat Anti-Rabbit IgG (H+L) (AS074, ABclonal) was selected as the secondary antibody. Images were collected using a Nikon fluorescence microscope.

Quantitative real-time PCR

Total RNA was extracted using MagicZol reagent and reverse transcribed using the 5X All-In-One RT Master-Mix kit (G490, abm). Besides, 2X Universal SYBR Green Fast qPCR Mix kit (RK21204, ABclonal) was used for quantitative real-time PCR. Also, β-actin was used as an internal control and $2^{-\Delta\Delta C_t}$ was applied to calculate the relative expression of the target gene. The analyzed genes and the primer sequences are listed in Table 1.

Western blot analysis

Total protein was extracted from primary microglia. The samples were lysed in RIPA buffer (P0013C, Beyotime) containing protease and phosphatase inhibitors. The BCA protein concentration assay kit (BL521A, Biosharp) was used for quantification. The protein was denatured at 100 °C, loaded on a 10% SDS-PAGE gel (P0012A, Beyotime), separated by electrophoresis, and transferred to a polyvinylidene fluoride PVDF membrane (IPVH00010, Immobilon) by wet transfer. After blocking with 5% milk for 1 h at room temperature, the Sirt6 (13572-1-AP, Proteintech) and β-actin (AP0060, Bioword) primary antibodies were used. After secondary antibody (ab205718, Abcam) incubation, detection was performed in a Bio-Rad chemiluminescence imager using the NcmECL ultra-sensitive ECL chemiluminescence kit (P10300, NCM Biotech, Suzhou, China). Quantitative analysis was performed using ImageJ software.

RNA sequencing

BV2 cells were treated with Adenoviruses Ad-Sirt6 or Ad-GFP for 12 h and then stimulated with OA and PA for 24 h. Total RNA was extracted with MagicZol reagent and RNA quality was detected. After the RNA samples were qualified, a mRNA-seq library was constructed. The library was quality-checked using Qubit 3.0, and PE150 sequencing was performed using the Illumina Nova-Seq6000 high-throughput sequencing platform. Next, basic data quality control was performed on the data

Table 1 Primer sequences used for the qPCR analysis

Gene	Forward Primer (5'-3')	Reverse Primer (5'-3')
<i>β-actin</i>	GGCTGTATCCCTCCATCG	CCAGTTGGTAACAATGCCATGT
<i>Sirt6</i>	ATGTCGGTGAATTATGCAGCA	GCTGGAGGACTGCCACATTA
<i>Ptp1b</i>	GGAACTGGGGCGCTATTTACC	CAAAAGGGCTGACATCTCGGT
<i>Lepr</i>	TGGTCCCAGCAGCTATGGT	ACCCAGAGAAGTTAGCACTGT
<i>Pi3k</i>	ACACCACGGTTTGGACTATGG	GGCTACAGTAGTGGGCTTGG
<i>Jak2</i>	TTGTGGTATTACGCTGTGTATC	ATGCCTGGTTGACTCGTCTAT
<i>Socs3</i>	ATGGTCACCCACAGCAAGTTT	TCCAGTAGAATCCGCTCTCCT
<i>Tnf-α</i>	CCCTCACACTCAGATCATCTTCT	GCTACGACGTGGGCTACAG
<i>Il-6</i>	TAGTCTTCTACCCCAATTTCC	TTGGTCTTAGCCACTCCTTC
<i>Il-1β</i>	GCAACTGTTCTGAACTCAACT	ATCTTTTGGGGTCCGTCACACT
<i>Cd16</i>	CAGAATGCACACTCTGGAAGC	GGGTCCCTTCGCACATCAG
<i>Cd86</i>	TGTTTCCGTGGAGACGCAAG	TTGAGCCTTTGTAAATGGGCA
<i>Ym1/2</i>	CAGGGTAATGAGTGGGTTGG	CACGGCACCTCTAAATTGT

obtained by sequencing. Specifically, the base sequences (reads) generated by the platform were quality filtered to obtain high-quality clean reads. The clean reads were then aligned to the SILVA database using bowtie2 software to remove rRNA, and the remaining reads were used for subsequent analysis. Then, the rRNA-free reads were aligned to the reference genome using Hisat2 software, and the gene expression level and gene structure were analysed. Additionally, heatmaps were generated using the R package hierarchical clustering algorithm.

Molecular docking

Since both receptor and ligand proteins are rigid, a rigid docking scheme was used to predict the binding mode between the Sirt6 and NRF2 proteins. From the protein database (<https://www.rcsb.org/>), the crystal structure of human Sirt6 protein/NAD-dependent deacetylase sirtuin-6 (Uniport ID: Q8N6T7) and nuclear factor erythroid 2-related factor 2/NRF2 (Uniport ID: Q14145) were retrieved with accession numbers 3K35 and 3ZGC, respectively. The initial complex structure was prepared by removing hydrogens, extra side chains, and extra ions, and minimization in PYMOL. Subsequently, rigid docking was achieved using the ZDOCK protocol. In Biovia Discovery Studio Server 2019, the modified protein structure-human Sirt6 protein/NAD-dependent deacetylase sirtuin-6 was set as the receptor protein and nuclear factor erythroid 2-related factor 2/NRF2 was the ligand protein. The docking protein structure was performed by Discovery Studio and the activity of the representative protein was predicted according to the docking results of the natural ligand protein (GFPT1, PDB ID: 2V4M).

Statistical analysis

Data were presented as mean \pm SEM. Statistical analysis was performed using GraphPad Prism version 8.4.0 software. Comparisons between two groups were analysed by the student's *t*-test, and a one-way or two-way ANOVA was used for comparison among multiple groups, followed by the Tukey post-hoc test. $P < 0.05$ denoted statistical significance.

Results

HFD reduces the expression of Sirt6 in mice hypothalamic microglia

To assess whether HFD affected the expression of Sirt6 in microglia, confocal experiments were used to observe the hypothalamus of mice exposed to either SD, 4 weeks of HFD, or 8 weeks of HFD. Ibal was selected as a biomarker of microglia. The results showed that HFD triggered hypothalamic microglial activation. Moreover, compared to the SD group, 8 weeks of HFD exposure induced a mild decrease of Sirt6 in the hypothalamic microglia (Fig. 1A). We further measured the mRNA expression

level of *Sirt6* in primary microglia of male mice on a HFD for 24 weeks. As expected, mRNA expression level of *Sirt6* were lower in mice on a HFD (Fig. 1B). Similarly, Sirt6 protein expression level was also lower in OA&PA-treated primary microglia of one-day-old neonatal mice (Fig. 1C).

Sirt6 knockout in microglia exacerbates high-fat diet-induced obesity in mice

To explore the effects of microglia Sirt6 on body weight and glucose homeostasis of mice fed with HFD, we measured indicators of body fat and glucose metabolism. First, SIRT6^{Mic^{-/-}} mice were produced by mating SIRT6^{fl/fl} mice with Cx3cr1-Cre mice. The result of the knockout was confirmed by gene identification (Additional file 1: S1A) and fluorescence microscopy (Additional file 1: S1B). Knockout of microglia Sirt6 resulted in a significant increase in the body weight of mice after a 12-week HFD (Fig. 2A). Similarly, the liver-to-bodyweight ratio of microglia Sirt6 knockout mice slightly increased after a 12-week HFD, but the difference was negligible (Fig. 2B). As predicted, SIRT6^{Mic^{-/-}} mice after a 12-week HFD exhibited significantly greater hepatic lipid accumulation and worse hepatic steatosis (Fig. 2C). Additionally, the adipose tissue of mice after a 12-week HFD also increased substantially, which was confirmed through the MicroCT images of inguinal white adipose tissue and epididymal white adipose tissue (iWAT and eWAT; Fig. 2D), different adipose tissue weights (Fig. 2E), and HE staining of the tissue cells (Fig. 2F). In the overnight fasted SIRT6^{Mic^{-/-}} group, insulin levels significantly increased (Fig. 2G). Moreover, GTT, ITT, and PTT results of mice after a 12-week HFD indicated abnormal glucose homeostasis (Fig. 2H-J). In comparison, in the standard chow diet, the body weight of microglia Sirt6 knockout mice slightly increased, but the difference was negligible (Additional file 2: S2A). Similarly, weights of different adipose tissue in mice mildly increased, but the differences were negligible (Additional file 2: S2B). However, HE staining of the histiocytes exhibited Sirt6 knockdown of microglia resulted in hypertrophy of iWAT (Additional file 2: S2C). Moreover, microglia Sirt6 knockout also resulted in abnormal ITT and PTT (Additional file 2: S2D-F). Thus, the data suggested that knockout of Sirt6 in microglia exacerbates high-fat diet-induced obesity in mice.

Sirt6 knockout in microglia leads to leptin resistance in mice

To determine the effect of Sirt6 knockout on leptin function, *Ptp1b*, *Lepr*, *Pi3k*, *Jhak2*, and *Socs3* were selected as biomarkers (Zabolotny et al. 2002). The results showed that the expression of the *Ptp1b* gene rose, while the expression of the *Pi3k* gene fell substantially, which implied that leptin-mediated appetite-suppressing

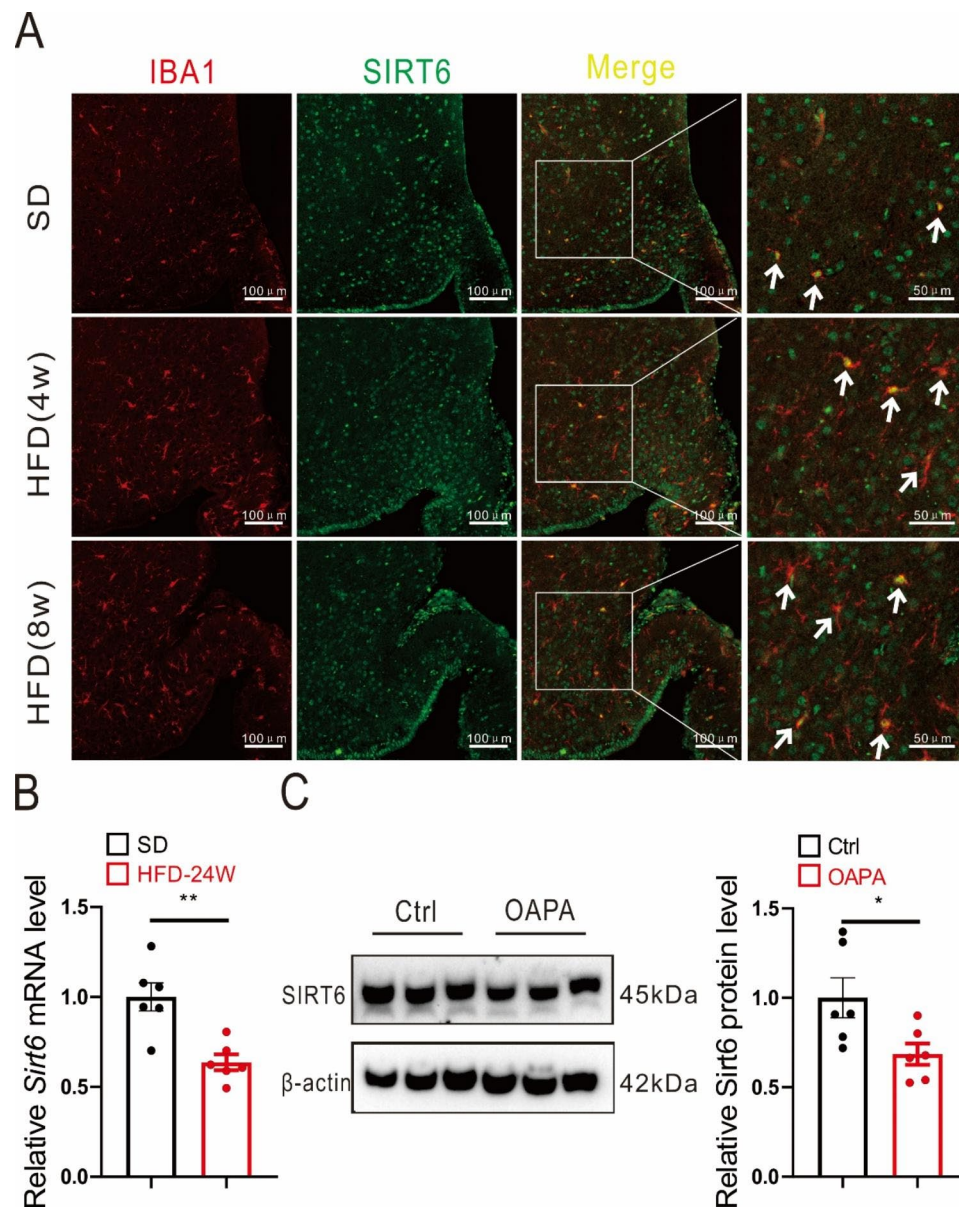


Fig. 1 Sirt6 responds to changes in the HFD environment. **A** Confocal images of Iba1 (red) and Sirt6 (green) in the hypothalamus after 4 and 8 weeks of HFD. Arrowheads indicate representative cells showing Iba1-positive cells. Scale bars: 100 μ m. **B** *Sirt6* mRNA expression level in microglia of male mice on a HFD for 24 weeks. Unpaired t-test. $n=6$ /group. **C** Sirt6 protein expression level in primary microglia of one-day-old neonatal mice after OA&PA treatment for 24 h. Unpaired t-test. $n=6$ /group. Data are presented as mean \pm SEM, * $p < 0.05$, ** $p < 0.01$

function was altered (Fig. 3A). Subsequently, we injected 1% BSA or leptin into mice and observed the fluorescence images of P-STAT3 (Ser727) in the hypothalamus. We observed inhibited activation of P-STAT3 (Ser727) in the *SIRT6*^{Mic^{-/-}} mice hypothalamus, which suggested that knockout of Sirt6 inhibited the function of leptin (Fig. 3B). This finding was also confirmed by the quantitative analysis of immunofluorescent intensity of P-STAT3 (Ser727) (Fig. 3C). Next, we determined the effect of Sirt6 knockout on food intake and body weight. Sirt6 knockout eliminated leptin-mediated food intake resistance (Fig. 3D), while food intake and body

weight were noticeably higher than in the control groups (Fig. 3E-F). Collectively, the results indicated that knockout of microglia Sirt6 led to leptin resistance.

Microglia Sirt6 deficiency leads to reduced energy expenditure in high-fat diet-fed mice

We further explored the effect of Sirt6 knockout on thermogenesis and body temperature in mice with a HFD. Sirt6 knockdown of microglia resulted in an increased volume but 'albino' morphology of brown adipose tissue in mice. Besides, the expression of UCP1-positive brown adipose cells decreased (Fig. 4A) and the norepinephrine

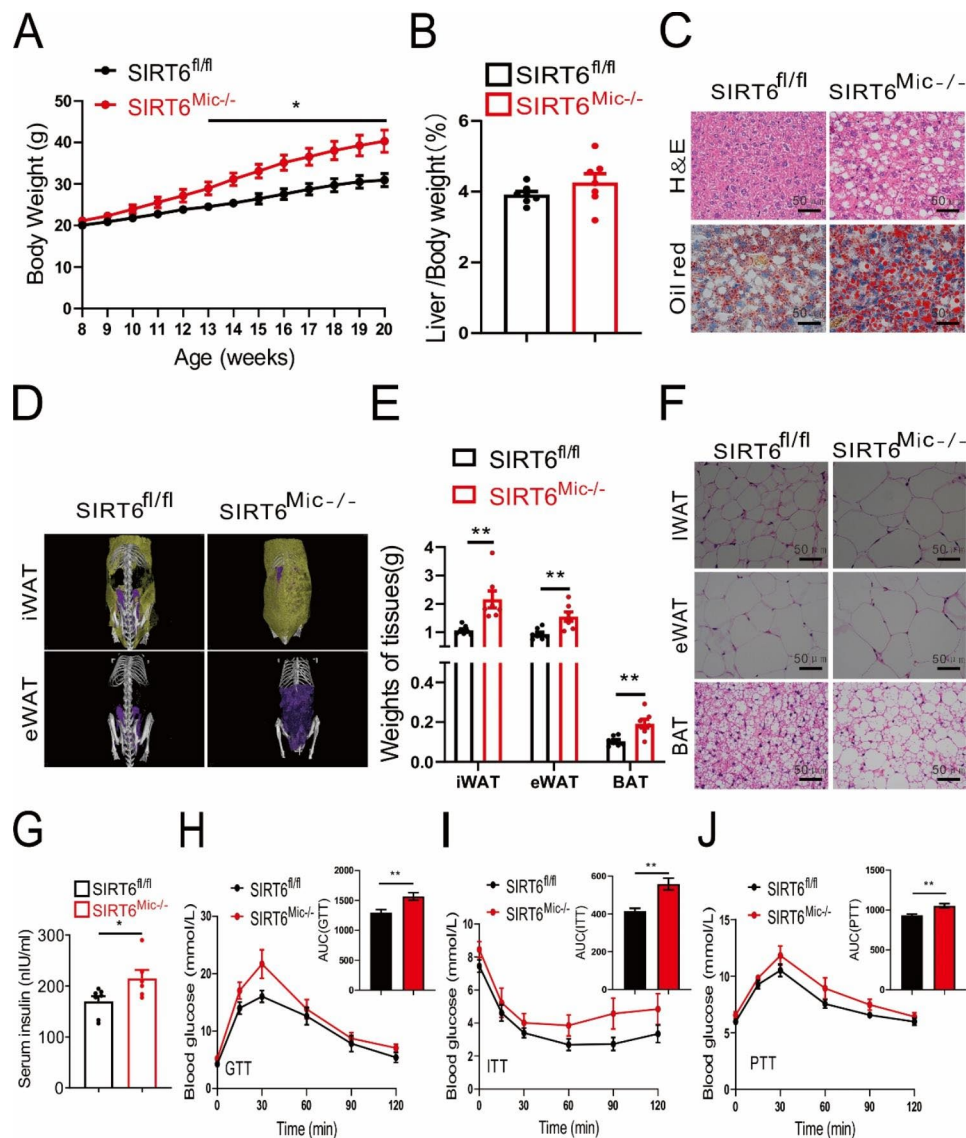


Fig. 2 Microglia *Sirt6* knockout mice are more prone to obesity after a 12-week HFD. **A** The growth curve of male mice on a HFD for 12 weeks. $n=7$ /group. **B** Liver-to-bodyweight ratio of male mice after a 12-week HFD. $n=7$ /group. **C** HE and oil red stain of liver cells of male mice after a 12-week HFD. Scale bars: 50 μm . **D** MicroCT image of iWAT and eWAT of male mice after a 12-week HFD. **E** Tissue weight of iWAT, eWAT, and BAT of male mice after a 12-week HFD. $n=7$ /group. **F** HE staining of iWAT, eWAT, and BAT of male mice after a 12-week HFD. Scale bars: 50 μm . **G** Serum insulin level in overnight fasted male mice after a 12-week HFD. $n=6-7$ /group. **H** Glucose tolerance test result of male mice after a 12-week HFD. $n=7$ /group. **I** Insulin tolerance test result of male mice after a 12-week HFD. $n=7$ /group. **J** Pyruvate tolerance test result of male mice after a 12-week HFD. $n=7$ /group. Data are presented as mean \pm SEM, * $p < 0.05$, ** $p < 0.01$

content in serum fell significantly (Fig. 4B). However, in the standard chow diet, norepinephrine content remained constant (Additional file 3: S3A). As anticipated, the core body temperature of the *Sirt6* knockout group was lower than the control group at the beginning and it decreased further when the mice were exposed to acute cold temperature (Fig. 5C). During this exposure, oxygen consumption, CO_2 production, and heat production of the mice also dropped significantly (Fig. 5D-F). However, there was no significant difference in the respiratory exchange ratio (RER) of the *Sirt6* knockout

and control groups, indicating that the decrease was not induced by locomotor activity (Additional file 3: S3B).

***Sirt6* deficiency in microglia exacerbates high-fat diet-induced hypothalamic inflammation in mice**

A HFD triggers hypothalamic inflammatory response before the body weight changes, so we further explored the effect of *Sirt6* knockout on high-fat diet-induced hypothalamic inflammatory response. Immunofluorescent localization results indicated that $\text{TNF-}\alpha$ was highly expressed in microglial cells (Fig. 5A). This finding was

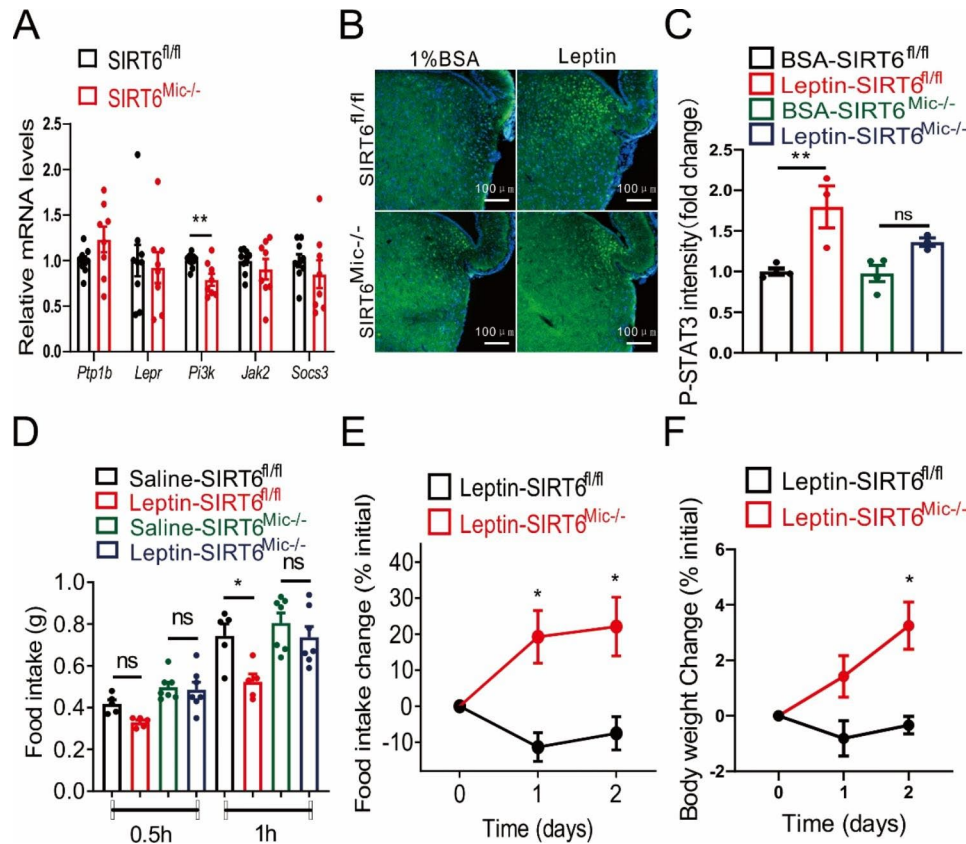


Fig. 3 Regulation of food intake by microglia Sirt6 correlates with leptin function. **A** mRNA expression of leptin signalling in the hypothalamus of male mice under a HFD for 8 weeks. $n=8-9$ /group. **B** Fluorescence images of P-STAT3 (Ser727) in the hypothalamus of mice after injection of 1% BSA or leptin (1 μ g/g) for 45 min. Scale bars: 100 μ m. **C** Quantitative analysis of immunofluorescent intensity of P-STAT3 (Ser727) in the hypothalamus of mice after injection of 1% BSA or leptin (1 μ g/g) for 45 min. $n=3-4$ /group. **D** Food intake change 1 h after leptin injection. $n=5-7$ /group. **E** Food intake change 2 days after leptin injection. $n=5$ /group. **F** Changes in body weight after leptin injection. $n=5$ /group. **C**, **D** Two-way ANOVA analysis followed by the Tukey post hoc test were performed. Data are presented as mean \pm SEM, * $p < 0.05$, ** $p < 0.01$

also confirmed by the statistical counting of TNF- α positive microglia (Fig. 5B). Moreover, Sirt6 knockout led to increased mRNA expression of *Tnf- α* , *Il-6* and *Il-1 β* in hypothalamus of male mice after a 8-week HFD (Fig. 5C). In comparison, for the standard diet, no significant differences in hypothalamic microglial number and size were observed between SIRT6^{fl/fl} and SIRT6^{Mic^{-/-}} mice (Additional file 4: S4A). Moreover, no significant differences in mRNA expression of inflammatory factors were observed between SIRT6^{fl/fl} and SIRT6^{Mic^{-/-}} mice (Additional file 4: S4B). Thus, the data suggested that Sirt6 deficiency in microglia exacerbated high-fat diet-induced hypothalamic inflammation.

Sirt6 overexpression ameliorates inflammation in BV2 cells

To investigate the regulation of Sirt6 on microglia polarity and its effect on inflammation, we measured the changes in microglial M1/M2 polarity surface markers and inflammation cytokines in BV2 cells. CD16, CD86, and CD68 were selected as biomarkers of M1 polarization, while YM1/2 were chosen as the biomarkers of M2

polarization. Besides, TNF- α , IL-6, and IL-1 β were chosen as the inflammatory cytokines (Balkwill et al. 2009; Tanaka et al. 2014; Tang et al. 2018; Zheng et al. 2020; Lopez-Castejon and Brough 2011). First, the results of sirt6 overexpression and sirt6 knockdown in BV2 cells were confirmed by Quantitative Real-Time PCR (Additional file 5: S5A-B). The results showed that the down-regulation of Sirt6 led to the M1 polarization state of BV2 cells (Fig. 6A). Conversely, overexpression of Sirt6 resulted in the M2 polarization state of BV2 cells (Fig. 6B). In BV2 cells, OA&PA treatment dramatically increased the mRNA expression levels of inflammatory factors, while overexpression of Sirt6 significantly reduced their expression (Fig. 6C). These results were also confirmed by the content of inflammatory cytokines in the culture medium (Fig. 6D) and immunofluorescence images (Fig. 6E-H).

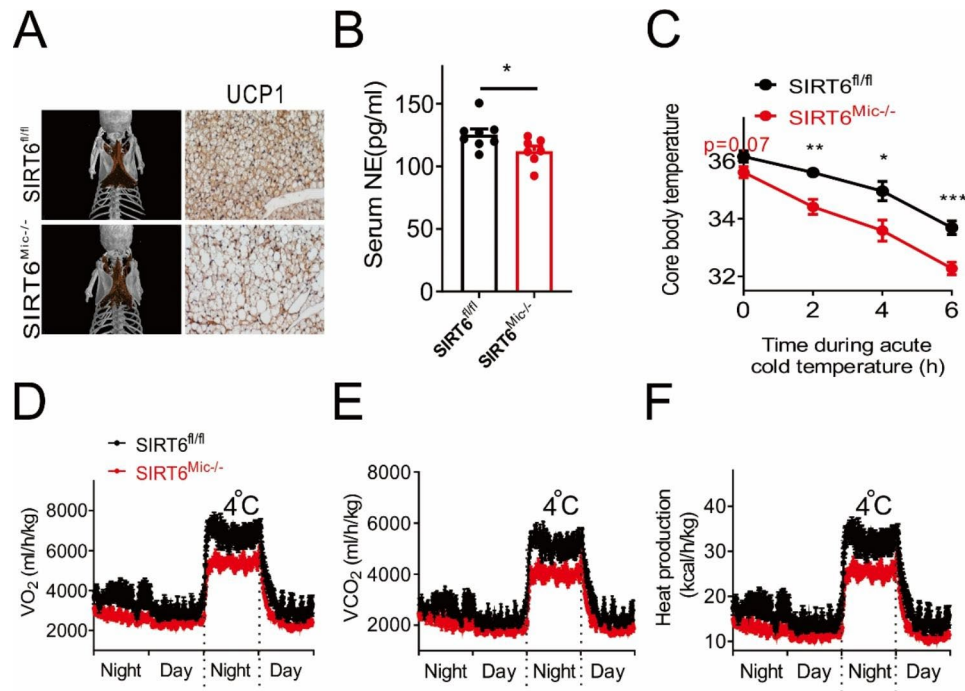


Fig. 4 Energy expenditure in high-fat diet-fed mice with *Sirt6* deficiency in microglia. **A** Images of brown fat and UCP1 immunohistochemical staining. **B** Serum NE content. $n=7-8$ /group. **C** Body core temperature of mice during acute cold exposure. $n=7$ /group. **D** Oxygen consumption of mice exposed to acute cold temperature. $n=5-6$ /group. **E** CO_2 production of mice exposed to acute cold temperature. $n=5-6$ /group. **F** Heat production of mice exposed to acute cold temperature. $n=5-6$ /group. Data are presented as mean \pm SEM, * $p < 0.05$, ** $p < 0.01$, *** $p < 0.001$

Sirt6 overexpression significantly increases NRF2 expression in BV2 cells

We further studied the mechanism of the *Sirt6* effect on the expression of inflammatory factors. Differential expression analysis using the RNA-seq data revealed that the downstream signalling pathway of *Sirt6* was associated with antioxidants (Fig. 7A). Correspondingly, antioxidant gene expression significantly increased in BV2 cells after overexpression of *Sirt6* (Fig. 7B). Conversely, antioxidant gene expression significantly decreased in BV2 cells after Knockdown of *Sirt6* (Fig. 7C). Since *Nrf2* is a crucial gene that senses oxidation and regulates anti-oxidation (Friedmann Angeli and Meierjohann 2021), we hypothesised that *Nrf2* was a key gene in the downstream pathway of *Sirt6*. As forecast, the Co-IP experiment demonstrated that *Sirt6* interacted with NRF2 in BV2 cells (Fig. 7D). Meanwhile, molecular docking showed that *Sirt6* and NRF2 had binding sites (Fig. 7E), and overexpression of *Sirt6* significantly increased the expression of NRF2 in BV2 cells (Fig. 7F). Moreover, immunofluorescence imaging also confirmed that *Sirt6* overexpression led to an increase in NRF2 expression (Fig. 7G-H). *Sirt6* is a member of the SIRT family (class III HDAC), which are highly conserved NAD^+ -dependent deacetylases. We constructed a *Sirt6*-overexpressing virus with deficient HDAC enzyme activity to verify whether the loss of HDAC enzyme activity influenced the anti-inflammatory and antioxidant effects of *Sirt6*. The results showed that

overexpression of *Sirt6* without HDAC enzyme activity eliminated the effect of *Sirt6* on Nfkb-p5 and $\text{TNF-}\alpha$ (Additional file 6: S6A-B), as well as the antioxidant genes *Gclm* and *Gclc* (Additional file 6: S6C-D).

NRF2 antagonists counteract *Sirt6* function in BV2 cells

To further verify that *Sirt6* reduced the expression of inflammatory factors through the NRF2 pathway, we used antagonists to inhibit NRF2 and measured the effect of *Sirt6* on inflammatory gene expression. Immunofluorescence results showed that after ML-385 blocked NRF2 expression, overexpression of *Sirt6* had no significant effect on the expression of Nfkb-p5 , CD68, and $\text{TNF-}\alpha$ (Fig. 8A-B). Furthermore, inflammatory cytokine content and mRNA expression of inflammatory genes exhibited no significant difference (Fig. 8C-D). Subsequently, we further determined the ROS content. As anticipated, ROS content showed no significant difference in the *Sirt6* overexpression group after NRF2 was blocked (Fig. 8E). Moreover, mRNA expression of *Gclm* and *Sod2* showed a negligible difference in the *Sirt6* overexpression group after NRF2 antagonist treatment (Fig. 8F).

Discussion

Microglia maintain synaptic remodelling, neurogenesis, and elimination of unwanted neurons and cellular debris, thereby promoting inner brain tissue homeostasis and

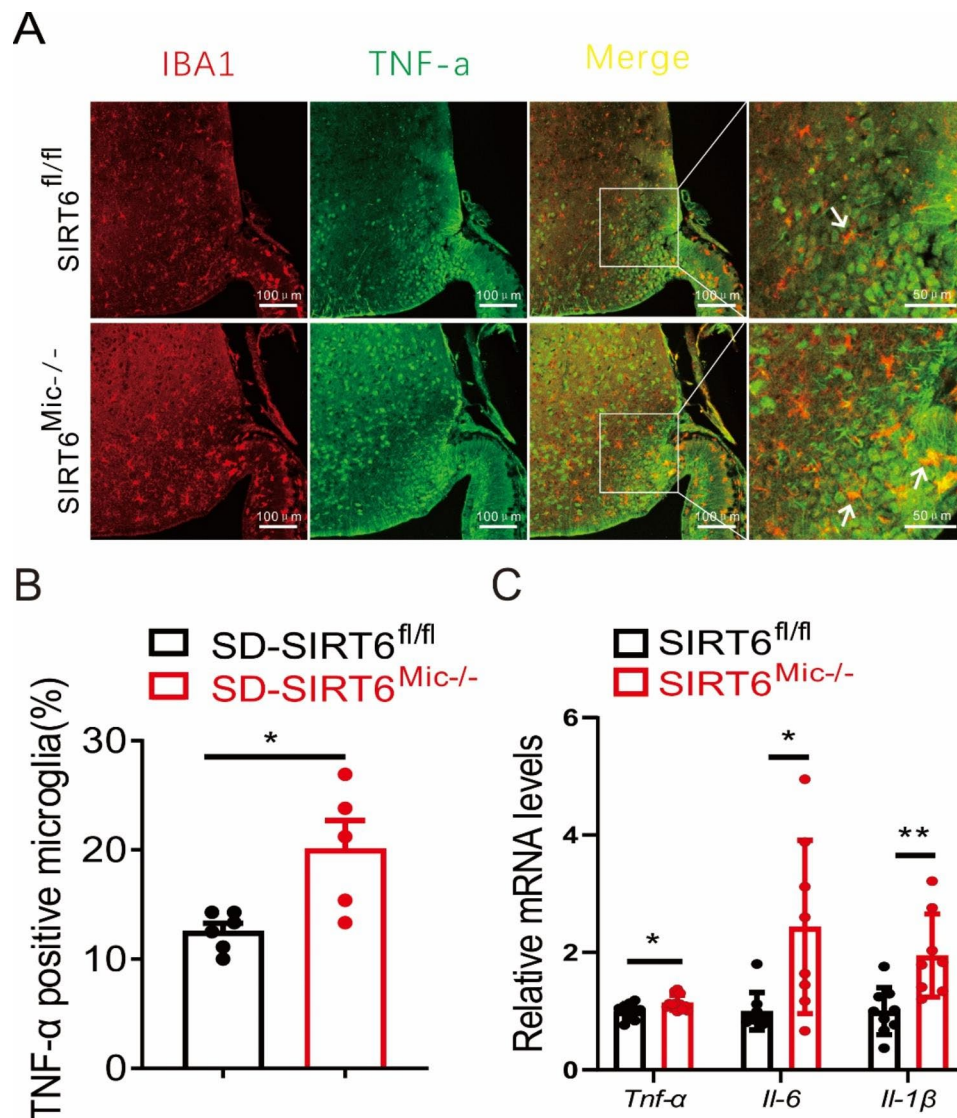


Fig. 5 Sirt6 deficiency in microglia exacerbates high-fat diet-induced hypothalamic inflammation. **A** Immunofluorescent localization of Iba1 (red) and TNF- α (green) in hypothalamus. Arrowheads indicate representative cells showing co-localization. Scale bars: 100 μ m. **B** TNF- α positive microglia counting from mice on a HFD for 12 weeks. $n=5-6$ /group. **C** mRNA expression of inflammatory factors in the hypothalamus of male mice on a HFD for 8 weeks. $n=8-12$ /group. Data are presented as mean \pm SEM, * $p < 0.05$, ** $p < 0.01$

regulating energy metabolism. This balance can be interrupted by high-fat diet-induced chronic inflammation. However, the specific mechanism of this process remains unknown (Wang et al. 2021). In this study, we found that Sirt6 was crucial in maintaining microglia function. Sirt6 ameliorated long-term high-fat diet-induced obesity, altered microglia polarity, and alleviated the inflammatory response in the hypothalamus. These processes were accomplished by the deacetylation of NRF2 by Sirt6 in microglia.

A HFD can cause a state of inflammation occurs in the hypothalamus (Alexaki 2021). As the resident immune cells of the brain, microglia transform into pro-inflammatory (M1) phenotype in the context of HFD. Inhibiting

microglia expansion hinders diet-induced body weight gain while preventing hypothalamic and peripheral inflammation due to caloric overload (André et al. 2017). Several studies have demonstrated that the transition of microglia from M1 to M2 can be mediated by multiple mechanisms. For instance, M2 microglia polarization is promoted by SIRT1, which reduces ROS-mediated NLRP3 inflammasome signalling (Xia et al. 2021). Existing research has proved that Sirt6 eliminated inflammatory response in the brain, as mentioned above (He et al. 2021). In this study, we first explored the effect of Sirt6 in protecting microglia. Our data showed that long-term HFD reduced Sirt6 expression of microglia in the hypothalamic region. Knockout of microglia Sirt6 exacerbated

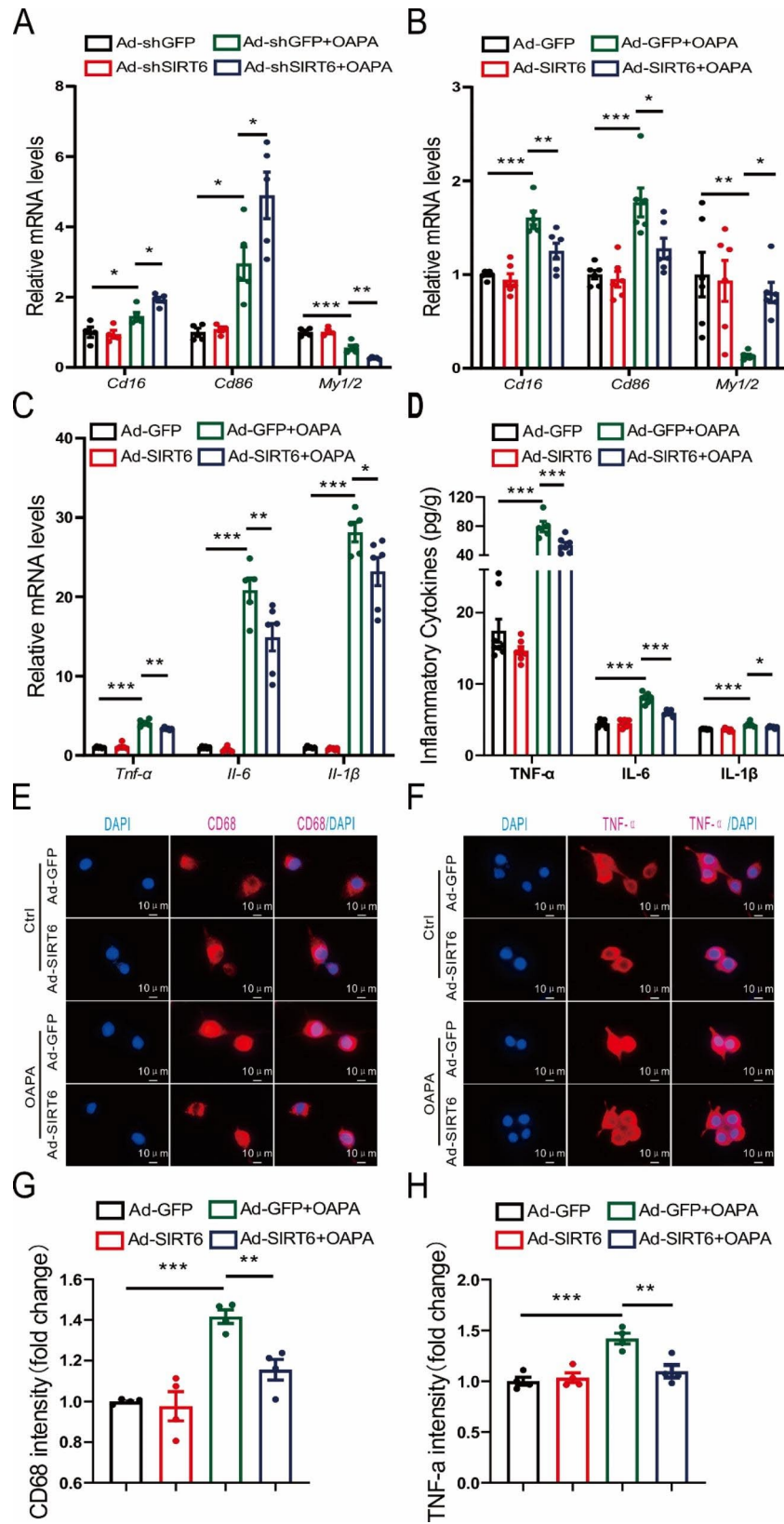


Fig. 6 Effect of Sirt6 on the inflammation of BV2 cells treated with OA&PA for 24 h. **A** Expression of M1-type microglia surface markers (*Cd16*, *Cd86*) and M2-type microglia surface markers (*Ym1/2*) in BV2 cells while Sirt6 was knocked down. **B** Expression of M1-type microglia surface markers (*Cd16*, *Cd86*) and M2-type microglia surface markers (*Ym1/2*) in BV2 cells while Sirt6 was over-expressed. **C** mRNA levels of *Tnf-α*, *Il-6*, and *Il-1β* in BV2 cells while Sirt6 was over-expressed. **D** Inflammatory cytokine (TNF-α, IL-6, and IL-1β) content in culture medium while Sirt6 was over-expressed. **E, F** Immunofluorescence images of CD68 and TNF-α while Sirt6 was over-expressed. Scale bars: 10 μm. **G, H** Quantitative analysis of immunofluorescent intensity of CD68 and TNF-α while Sirt6 was over-expressed. **A-D, G-H** Two-way ANOVA analysis was performed, followed by the Tukey post hoc test. $n = 4-8$ /group. Data are presented as mean \pm SEM, * $p < 0.05$, ** $p < 0.01$, *** $p < 0.001$

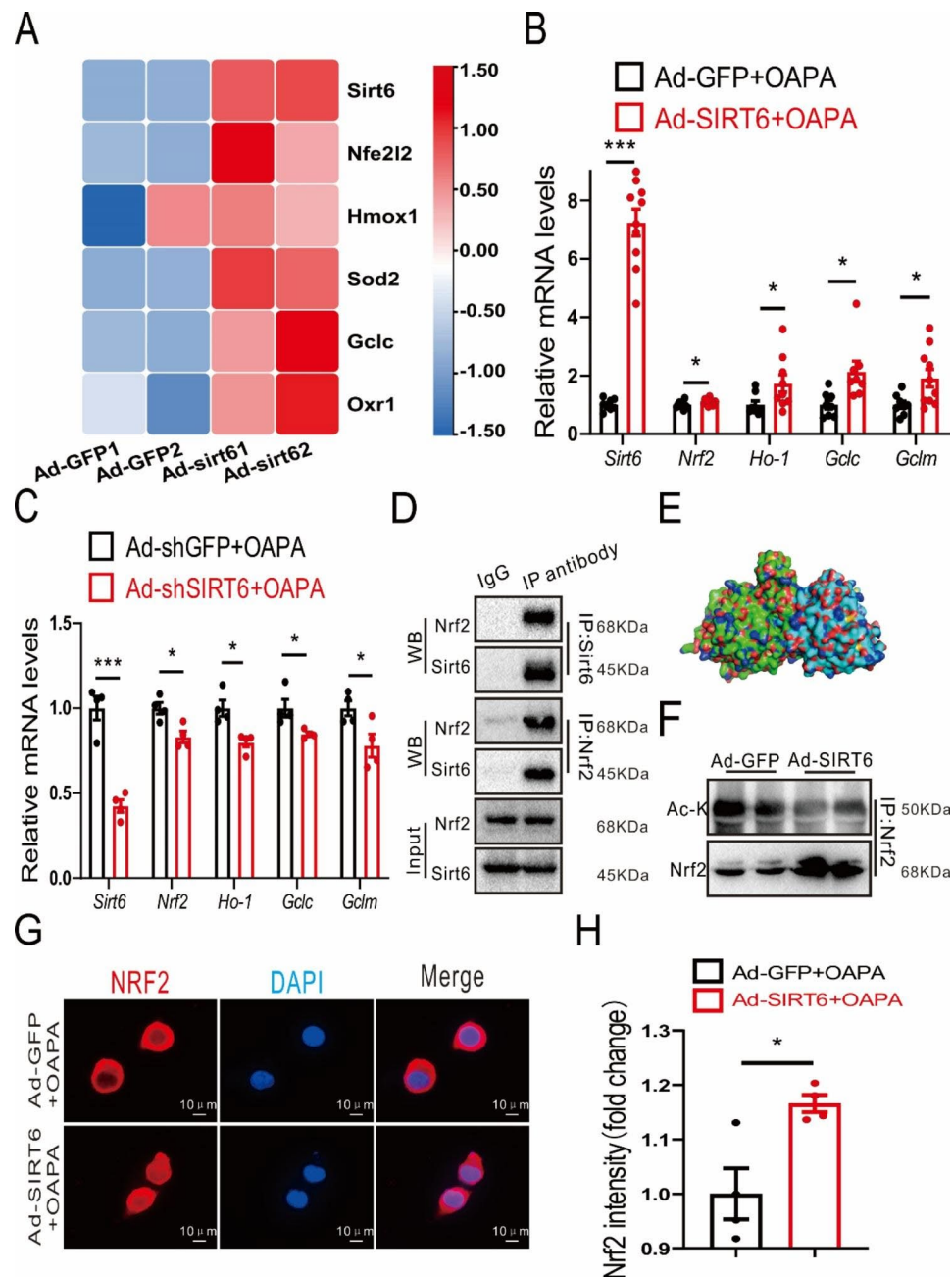


Fig. 7 Interaction of Sirt6 with NRF2. **A** Transcriptome screening for antioxidation. $n=2$ /group. **B** Overexpression of Sirt6 increases mRNA expression of antioxidant genes *Nrf2*, *Ho-1*, *Gclc*, and *Gclm* in BV2 Cells. $n=8-12$ /group. **C** Knockdown of Sirt6 decreases mRNA expression of antioxidant genes *Nrf2*, *Ho-1*, *Gclc*, and *Gclm* in BV2 Cells. $n=4$ /group. **D** Co-IP results verify that Sirt6 interacts with NRF2 in BV2 Cells. **E** Molecular docking of Sirt6 and NRF2 protein. **F** Effect of Sirt6 overexpression on NRF2 in BV2 Cells. **G** Immunofluorescence images of NRF2 while Sirt6 was over-expressed in BV2 Cells. Scale bars: 10 μ m. **H** Quantitative analysis of immunofluorescent intensity of NRF2 while Sirt6 was over-expressed in BV2 Cells. $n=4$ /group. Data are presented as mean \pm SEM, * $p < 0.05$, *** $p < 0.001$

high-fat diet-induced hypothalamic microglial activation and inflammation. Conversely, further experiments in vitro proved that Sirt6 overexpression shifted microglia polarity and moderated inflammation. Collectively, Our data suggested that Sirt6 may have a key role in protecting microglia.

Furthermore, leptin is an adipocyte-derived hormone that contributes to the homeostatic regulation of energy balance and metabolism through humoral and neural pathways (Liu et al. 2018). Previous studies have shown that the basic mechanisms related to leptin resistance include: blood-brain barrier transporter disorder, competitive inhibition of leptin, mutations of LepR, and

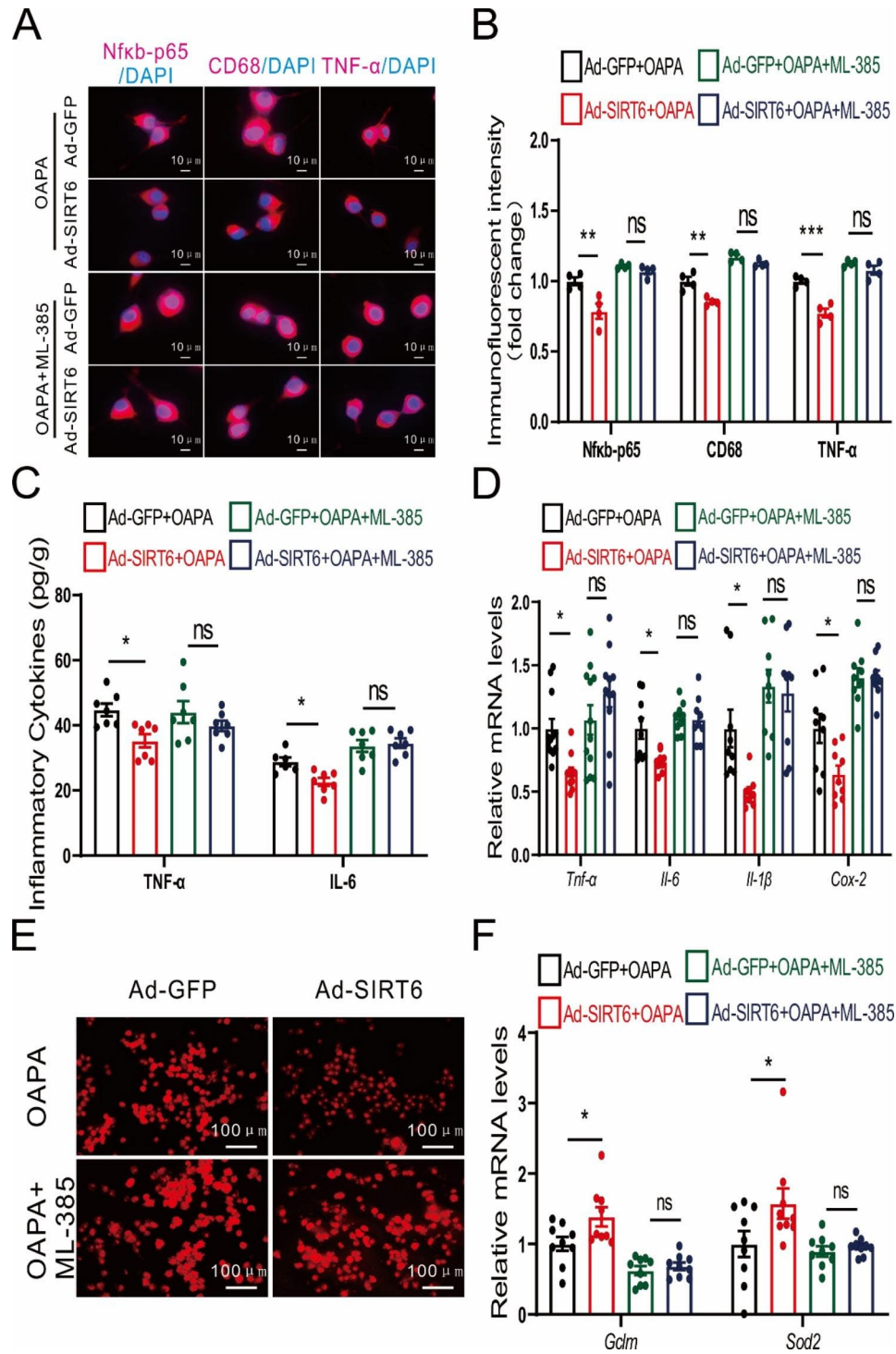


Fig. 8 NRF2 antagonists counteract the ameliorating effects of Sirt6 on inflammation and oxidative stress. **A** Immunofluorescence images of Nfkb-p65, CD68, and TNF- α in BV2 cells with combined Sirt6 overexpression and NRF2 antagonist treatment. Scale bars: 10 μ m. **B** Quantitative analysis of immunofluorescent intensity of Nfkb-p65, CD68, and TNF- α in BV2 cells with combined Sirt6 overexpression and NRF2 antagonist treatment. $n = 4$ /group. **C** Expression of inflammatory cytokines TNF- α and IL-6. $n = 6-7$ /group. **D** mRNA expression of *Tnf- α* , *Il-6*, *Il-1 β* , and *Cox-2*. $n = 9-12$ /group. **E** Immunofluorescence images of ROS. Scale bars: 100 μ m. **F** mRNA expression levels of *Gclm* and *Sod2*. $n = 9$ /group. **B-D, F** Two-way ANOVA analysis followed by the Tukey post hoc test were performed. ns: not significant. Data are presented as mean \pm SEM, * $p < 0.05$, ** $p < 0.01$, *** $p < 0.001$

impairment of leptin cellular signalling (Liu et al. 2018). Here, we demonstrated that knockout of *Sirt6* in microglia resulted in ineffective leptin-mediated appetite suppression and weight gain in mice. Similarly, Tang et al. found that *Sirt6* in pro-opiomelanocortin (POMC) neurons controlled energy metabolism by modulating leptin signalling (Tang et al. 2020). HFD has a significant effect on the cytoarchitecture of the arcuate nucleus, which may be irreversible due to reactive gliosis (Horvath et al. 2010). Our results revealed that knockout of *Sirt6* in microglia led to leptin resistance, which further confirmed *Sirt6* as a protector of microglia.

In addition to suppressing appetite, *Sirt6* also plays a key role in regulating fat thermogenesis (Kuang et al. 2018). In adipose tissue, *Sirt6* deletion moderates the binding of phosphorylated ATF2 to the PGC-1 α promoter, which subsequently reduces the thermogenic programme in brown fat and eventually leads to obesity (Yao et al. 2017). *Sirt6* is an important component of the CNS, and we discovered that its loss in hypothalamic microglia led to reduced energy expenditure, which was manifested by impaired brown cell function, lower body temperature in cold environments, and reduced energy expenditure. This process in turn led to weight gain and increased the liver-to-weight ratio and hypertrophy of white adipose tissue, ultimately resulting in obesity.

Sirt6 is also involved in the regulation of oxidative stress-related diseases (Tasselli et al. 2017; Chang et al. 2020). In tissue such as liver, human mesenchymal stem cells, and human lens epithelial cells, *Sirt6* cooperates with NRF2 to achieve antioxidant and anti-inflammatory effects (Zhou et al. 2021; Pan et al. 2016; Sun et al. 2019). For instance, *Sirt6* cooperates with NRF2 to attenuates APAP-induced hepatotoxicity by inhibiting oxidative stress (Zhou et al. 2021). *SIRT6* also protects human mesenchymal stem cells from oxidative stress via NRF2 (Pan et al. 2016). Moreover, activation of *SIRT6-Nrf2* signaling protects human lens epithelial cells from ultraviolet-induced oxidative damage (Sun et al. 2019). In this study, we revealed that in microglia, *Sirt6* overexpression improved inflammatory response and oxidative stress, and its mechanism was the deacetylation of NRF2. As mentioned above, NRF2 and its endogenous inhibitor, Keap1, function as a ubiquitous, evolutionarily conserved intracellular defence mechanism to counteract oxidative stress (Silva-Islas and Maldonado 2018; Bellezza et al. 2018). We found that *Sirt6* deacetylated and stabilised NRF2 to increase the expression of anti-oxidative genes and defend against ROS overload. Moreover, pharmacological inhibition of NRF2 eliminated the beneficial modulating effects of *Sirt6* on microglial activity. Our findings further elucidated the mechanism of the microglia *Sirt6* for oxidative stress and inflammatory responses, thereby providing novel insights into how the CNS defend against

obesity induced by a HFD. Collectively, this study of *Sirt6* in the energy regulation of microglia complements current knowledge on the mechanism by which *Sirt6* controls whole-body energy metabolism in the CNS.

Conclusion

Our results reveal that microglia *Sirt6* in the hypothalamus is essential in the regulation of metabolism and further prove that *Sirt6* plays an important role in high-fat diet-induced obesity via the manipulation of hypothalamic inflammatory response and energy expenditure. Therefore, microglial *Sirt6* may be an important therapeutic target for obesity.

Abbreviations

HFD	High-fat diet
PVN	Paraventricular nucleus
PFA	Perifornical area
LHA	Lateral hypothalamic area
ARC	Arcuate nucleus
DIO	Diet-induced obesity
CNS	Central nervous system
NRF2	Nuclear Factor Erythroid 2-related Factor 2
Keap1	Kelch-like ECH-associated Protein 1
ARE	Antioxidant Response Elements
SD	Standard chow diet
H&E	Hematoxylin and eosin
GTT	Glucose tolerance test
ITT	Insulin tolerance test
PTT	Pyruvate tolerance test
CLAMS	Comprehensive laboratory animal monitoring system
OA	Oleic acid
PA	Palmitic acid
ROS	Reactive oxygen species
POMC	Pro-opiomelanocortin

Supplementary Information

The online version contains supplementary material available at <https://doi.org/10.1186/s10020-023-00676-9>.

Additional file 1: S1 Confirmation of microglia *Sirt6* knockout mice. **A** Gene identification of microglia *Sirt6* knockout of mice. **B** Validation of *Sirt6* knockout mice by immunofluorescence. Scale bars: 100 μ m

Additional file 2: S2 Effects of microglia *Sirt6* knockout on body weight and glucose homeostasis of mice under a standard diet. **A** Body weight of *Sirt6* knockout mice on a standard diet. $n=6$ /group. **B** Tissue weight of iWAT, eWAT, and BAT. $n=6$ /group. **C** HE staining of iWAT, eWAT, and BAT. Scale bars: 50 μ m. **D-F** Results of GTT, ITT, and PTT tests in mice under the standard chow diet. $n=8$ /group. Data are presented as mean \pm SEM, ** $p < 0.01$, *** $p < 0.001$

Additional file 3: S3 Serum NE content and RER of microglia *Sirt6* knockout mice. **A** Serum NE content under a standard diet. $n=4-5$ /group. **B** RER result of mice fed with HFD exposed to acute cold temperature. Data are presented as mean \pm SEM

Additional file 4: S4 Expression of hypothalamic inflammation in male mice under a standard diet. **A** Fluorescence images of Iba1 in hypothalamus of male mice under a standard diet. Scale bars: 100 μ m. **B** mRNA expression of inflammatory factors in hypothalamus of male mice under a standard diet. $n=7-11$ /group. Data are presented as mean \pm SEM. ns: not significant.

Additional file 5: S5 Confirmation of *Sirt6* expression and knockdown. **A** mRNA expression level of *Sirt6* in BV2 cells while *Sirt6* was over-expressed. **B** mRNA expression level of *Sirt6* in BV2 cells while *Sirt6* was knocked

down. **A, B** Welch's t-test. $n=6/\text{group}$. Data are presented as mean \pm SEM, ** $p < 0.01$, *** $p < 0.001$

Additional file 6: S6 Effect of Sirt6 without HDAC enzyme activity on the inflammation and antioxidation of BV2 cells treated with OA&PA for 24 h. **A** Overexpression of Sirt6 without HDAC enzyme activity eliminates the effect of Sirt6 on Nfkb-p65. Scale bars: 10 μm . **B** Overexpression of Sirt6 without HDAC enzyme activity eliminates the effect of Sirt6 on TNF- α . Scale bars: 100 μm . **C** mRNA expression level of *Gclc*. **D** mRNA expression level of *Gclm*. **C, D** One-way ANOVA analysis followed by the Tukey post hoc test were performed. $n=7-8/\text{group}$. Data are presented as mean \pm SEM, * $p < 0.05$, *** $p < 0.001$

Acknowledgements

The authors wish to thank Science and Technology Innovation Center, Guangzhou University of Chinese Medicine for providing experimental platform.

Authors' contributions

Conceptualization, Q.W., Y.G. and X.X.X.; methodology, X.X.X., Y.D.Z., Y.J.C. and K.J.T.; software, X.X.X. and Y.D.Z.; validation, X.X.X., H.L.H. and X.Y.Y.; formal analysis, X.X.X. and H.L.H.; investigation, Z.S.P., K.J.T. and X.X.X.; resources, Y.G. and Q.W.; data curation, Y.G. and X.X.X.; writing—original draft preparation, H.L.H. and X.X.X.; writing—review and editing, Q.W., Y.G., X.Y.Y. and X.X.X.; visualization, X.X.X. and J.W.H.; supervision, Q.W., Y.G. and X.Y.Y.; project administration, Q.W. and Y.G.; funding acquisition, Q.W. and Y.G. All authors have read and agreed to the published version of the manuscript.

Funding

This work was supported by National Natural Science Foundation of China (82000803), Guangdong Basic and Applied Basic Research Foundation (2019A1515010980) and the Key projects of Guangdong Provincial Department of Education (2021ZDZX2010).

Data Availability

Data will be made available on request.

Ethics approval and consent to participate

All animal handling complied with the guidelines of the Experimental Animal Ethics Committee of Guangzhou University of Chinese Medicine and the experimental protocol was approved.

Consent for publication

Not applicable.

Competing interests

The authors declare that they have no competing interests.

Received: 31 January 2023 / Accepted: 31 May 2023

Published online: 15 August 2023

References

- Alexaki VI. The impact of obesity on microglial function: Immune, metabolic and endocrine perspectives. *Cells*. 2021;10(7):1584. <https://doi.org/10.3390/cells10071584>.
- André C, Guzman-Quevedo O, Rey C, Rémus-Borel J, Clark S, Castellanos-Jankiewicz A, et al. Inhibiting Microglia Expansion prevents Diet-Induced Hypothalamic and Peripheral Inflammation. *Diabetes*. 2017;66(4):908–19. <https://doi.org/10.2337/db16-0586>.
- Balkwill F. Tumour necrosis factor and cancer. *Nat Rev Cancer*. 2009;9(5):361–71. <https://doi.org/10.1038/nrc2628>.
- Bellezza I, Giambanco I, Minelli A, Donato R. Nrf2-Keap1 signaling in oxidative and reductive stress. *Biochim Biophys Acta Mol Cell Res*. 2018;1865(5):721–33. <https://doi.org/10.1016/j.bbamcr.2018.02.010>.
- Chang AR, Ferrer CM, Mostoslavsky R. SIRT6, a mammalian deacetylase with multitasking abilities. *Physiol Rev*. 2020;100(1):145–69. <https://doi.org/10.1152/physrev.00030.2018>.
- Chausse B, Kakimoto PA, Caldeira-da-Silva CC, Yoshinaga MY, da Silva RP, et al. Distinct metabolic patterns during microglial remodeling by oleate and palmitate. *Biosci Rep*. 2019;39(4):BSR20190072. <https://doi.org/10.1042/BSR20190072>.
- Friedmann Angeli JP, Meierjohann S. NRF2-dependent stress defense in tumor antioxidant control and immune evasion. *Pigment Cell Melanoma Res*. 2021;34(2):268–79. <https://doi.org/10.1111/pcmr.12946>.
- He T, Shang J, Gao C, Guan X, Chen Y, Zhu L, et al. A novel SIRT6 activator ameliorates neuroinflammation and ischemic brain injury via EZH2/FOXO1 axis. *Acta Pharm Sin B*. 2021;11(3):708–26. <https://doi.org/10.1016/j.apsb.2020.11.002>.
- Horvath TL, Sarman B, García-Cáceres C, Enriori PJ, Sotonyi P, Shanabrough M, et al. Synaptic input organization of the melanocortin system predicts diet-induced hypothalamic reactive gliosis and obesity. *Proc Natl Acad Sci U S A*. 2010;107(33):14875–80. <https://doi.org/10.1073/pnas.1004282107>.
- Kanfi Y, Peshti V, Gil R, Naiman S, Nahum L, Levin E, et al. SIRT6 protects against pathological damage caused by diet-induced obesity. *Aging Cell*. 2010;9(2):162–73. <https://doi.org/10.1111/j.1474-9726.2009.00544.x>.
- Kuang J, Zhang Y, Liu Q, Shen J, Pu S, Cheng S, et al. Fat-Specific Sirt6 ablation sensitizes mice to High-Fat Diet-Induced obesity and insulin resistance by inhibiting Lipolysis. *Diabetes*. 2017;66(5):1159–71. <https://doi.org/10.2337/db16-1225>.
- Kuang J, Chen L, Tang Q, Zhang J, Li Y, He J. The role of Sirt6 in obesity and diabetes. *Front Physiol*. 2018;9:135. <https://doi.org/10.3389/fphys.2018.00135>.
- Lee Y, Ka SO, Cha HN, Chae YN, Kim MK, Park SY, et al. Myeloid sirtuin 6 Deficiency causes insulin resistance in High-Fat Diet-Fed mice by eliciting macrophage polarization toward an M1 phenotype. *Diabetes*. 2017;66(10):2659–68. <https://doi.org/10.2337/db16-1446>.
- Liberale L, Gaul DS, Akhmedov A, Bonetti NR, Nageswaran V, Costantino S, et al. Endothelial SIRT6 blunts stroke size and neurological deficit by preserving blood-brain barrier integrity: a translational study. *Eur Heart J*. 2020;41(16):1575–87. <https://doi.org/10.1093/eurheartj/ehz712>.
- Liu J, Yang X, Yu S, Zheng R. The Leptin Resistance. *Adv Exp Med Biol*. 2018;1090:145–63. https://doi.org/10.1007/978-981-13-1286-1_8.
- Lopez-Castejon G, Brough D. Understanding the mechanism of IL-1 β secretion. *Cytokine Growth Factor Rev*. 2011;22(4):189–95. <https://doi.org/10.1016/j.cytogfr.2011.10.001>.
- Martín-Montañez E, Valverde N, de Ladrón D, Lara E, Romero-Zerbo YS, Millon C, et al. Insulin-like growth factor II prevents oxidative and neuronal damage in cellular and mice models of Parkinson's disease. *Redox Biol*. 2021;46:102095. <https://doi.org/10.1016/j.redox.2021.102095>.
- Mendes NF, Kim YB, Velloso LA, Araujo EP. Hypothalamic microglial activation in obesity: a Mini-Review. *Front Neurosci*. 2018;12:846. <https://doi.org/10.3389/fnins.2018.00846>.
- Mostoslavsky R, Chua KF, Lombard DB, Pang WW, Fischer MR, Gellon L, et al. Genomic instability and aging-like phenotype in the absence of mammalian SIRT6. *Cell*. 2006;124(2):315–29. <https://doi.org/10.1016/j.cell.2005.11.044>.
- Nadal A, Quesada I, Tudurí E, Nogueiras R, Alonso-Madgalena P. Endocrine-disrupting chemicals and the regulation of energy balance. *Nat Rev Endocrinol*. 2017;13(9):536–46. <https://doi.org/10.1038/nrendo.2017.51>.
- Nakano-Kobayashi A, Fukumoto A, Morizane A, Nguyen DT, Le TM, Hashida K, et al. Therapeutics potentiating microglial p21-Nrf2 axis can rescue neurodegeneration caused by neuroinflammation. *Sci Adv*. 2020;6(46):eabc1428. <https://doi.org/10.1126/sciadv.abc1428>.
- Pan H, Guan D, Liu X, Li J, Wang L, Wu J, et al. SIRT6 safeguards human mesenchymal stem cells from oxidative stress by coactivating NRF2. *Cell Res*. 2016;26(2):190–205. <https://doi.org/10.1038/cr.2016.4>.
- Reis WL, Yi CX, Gao Y, Tschöp MH, Stern JE. Brain innate immunity regulates hypothalamic arcuate neuronal activity and feeding behavior. *Endocrinology*. 2015;156(4):1303–15. <https://doi.org/10.1210/en.2014-1849>.
- Rohwedder A, Zhang Q, Rudge SA, Wakelam MJ. Lipid droplet formation in response to oleic acid in Huh-7 cells is mediated by the fatty acid receptor FFAR4. *J Cell Sci*. 2014;127(14):3104–15. <https://doi.org/10.1242/jcs.145854>.
- Rojo AI, Pajares M, García-Yagüe AJ, Buendia I, Van Leuven F, Yamamoto M, et al. Deficiency in the transcription factor NRF2 worsens inflammatory parameters in a mouse model with combined tauopathy and amyloidopathy. *Redox Biol*. 2018;18:173–80. <https://doi.org/10.1016/j.redox.2018.07.006>.
- Schwartz MW, Woods SC, Porte D Jr, Seeley RJ, Baskin DG. Central nervous system control of food intake. *Nature*. 2000;404(6778):661–71. <https://doi.org/10.1038/35007534>.
- Silva-Islas CA, Maldonado PD. Canonical and non-canonical mechanisms of Nrf2 activation. *Pharmacol Res*. 2018;134:92–9. <https://doi.org/10.1016/j.phrs.2018.06.013>.
- Sun GL, Huang D, Li KR, Jiang Q. microRNA-4532 inhibition protects human lens epithelial cells from ultra-violet-induced oxidative injury via activating

- SIRT6-Nrf2 signaling. *Biochem Biophys Res Commun.* 2019;514(3):777–84. <https://doi.org/10.1016/j.bbrc.2019.05.026>.
- Sun N, Shen C, Zhang L, Wu X, Yu Y, Yang X, et al. Hepatic Krüppel-like factor 16 (KLF16) targets PPAR α to improve steatohepatitis and insulin resistance. *Gut.* 2021;70(11):2183–95. <https://doi.org/10.1136/gutjnl-2020-321774>.
- Tanaka T, Narazaki M, Kishimoto T. IL-6 in inflammation, immunity, and disease. *Cold Spring Harb Perspect Biol.* 2014;6(10):a016295. <https://doi.org/10.1101/cshperspect.a016295>.
- Tang J, Yu W, Chen S, Gao Z, Xiao B. Microglia polarization and endoplasmic reticulum stress in chronic social defeat stress Induced Depression mouse. *Neurochem Res.* 2018;43(5):985–94. <https://doi.org/10.1007/s11064-018-2504-0>.
- Tang Q, Gao Y, Liu Q, Yang X, Wu T, Huang C, et al. Sirt6 in pro-opiomelanocortin neurons controls energy metabolism by modulating leptin signaling. *Mol Metab.* 2020;37:100994. <https://doi.org/10.1016/j.molmet.2020.100994>.
- Tasselli L, Zheng W, Chua KF. SIRT6: novel mechanisms and links to Aging and Disease. *Trends Endocrinol Metab.* 2017;28(3):168–85. <https://doi.org/10.1016/j.tem.2016.10.002>.
- Thaler JP, Yi CX, Schur EA, Guyenet SJ, Hwang BH, Dietrich MO, et al. Obesity is associated with hypothalamic injury in rodents and humans. *J Clin Invest.* 2012;122(1):153–62. <https://doi.org/10.1172/JCI59660>.
- Valdearcos M, Robblee MM, Benjamin DI, Nomura DK, Xu AW, Koliwad SK. Microglia dictate the impact of saturated fat consumption on hypothalamic inflammation and neuronal function. *Cell Rep.* 2014;9(6):2124–38. <https://doi.org/10.1016/j.celrep.2014.11.018>.
- Valdearcos M, Xu AW, Koliwad SK. Hypothalamic inflammation in the control of metabolic function. *Annu Rev Physiol.* 2015;77:131–60. <https://doi.org/10.1146/annurev-physiol-021014-071656>.
- Valdearcos M, Douglass JD, Robblee MM, Dorfman MD, Stiffler DR, Bennett ML, et al. Microglial Inflammatory Signaling orchestrates the Hypothalamic Immune response to dietary excess and mediates obesity susceptibility. *Cell Metab.* 2017;26(1):185–197e183. <https://doi.org/10.1016/j.cmet.2017.05.015>.
- Wang XL, Li L. Microglia regulate neuronal circuits in homeostatic and High-Fat Diet-Induced Inflammatory Conditions. *Front Cell Neurosci.* 2021;15:722028. <https://doi.org/10.3389/fncel.2021.722028>.
- Xia DY, Yuan JL, Jiang XC, Qi M, Lai NS, Wu LY, et al. SIRT1 promotes M2 Microglia polarization via reducing ROS-Mediated NLRP3 Inflammasome Signaling after Subarachnoid Hemorrhage. *Front Immunol.* 2021;12:770744. <https://doi.org/10.3389/fimmu.2021.770744>.
- Yagishita Y, Fukutomi T, Sugawara A, Kawamura H, Takahashi T, Pi J, et al. Nrf2 protects pancreatic β -cells from oxidative and nitrosative stress in diabetic model mice. *Diabetes.* 2014;63(2):605–18. <https://doi.org/10.2337/db13-0909>.
- Yagishita Y, Urano A, Fukutomi T, Saito R, Saigusa D, Pi J, et al. Nrf2 improves leptin and insulin resistance provoked by hypothalamic oxidative stress. *Cell Rep.* 2017;18(8):2030–44. <https://doi.org/10.1016/j.celrep.2017.01.064>.
- Yao L, Cui X, Chen Q, Yang X, Fang F, Zhang J, et al. Cold-inducible SIRT6 regulates thermogenesis of Brown and Beige Fat. *Cell Rep.* 2017;20(3):641–54. <https://doi.org/10.1016/j.celrep.2017.06.069>.
- Zabolotny JM, Bence-Hanulec KK, Stricker-Krongrad A, Haj F, Wang Y, Minokoshi Y, et al. PTP1B regulates leptin signal transduction in vivo. *Dev Cell.* 2002;2(4):489–95. [https://doi.org/10.1016/s1534-5807\(02\)00148-x](https://doi.org/10.1016/s1534-5807(02)00148-x).
- Zhang J, Li Y, Liu Q, Huang Y, Li R, Wu T, et al. Sirt6 alleviated liver fibrosis by deacetylating conserved lysine 54 on Smad2 in hepatic stellate cells. *Hepatology.* 2021;73(3):1140–57. <https://doi.org/10.1002/hep.31418>.
- Zheng X, Gan H, Li L, Hu X, Fang Y, Chu L. Astragaloside IV inhibits inflammation after cerebral ischemia in rats through promoting microglia/macrophage M2 polarization. *Zhejiang Da Xue Xue Bao Yi Xue Ban.* 2020;49(6):679–86. <https://doi.org/10.3785/j.issn.1008-9292.2020.12.02>.
- Zhou Y, Fan X, Jiao T, Li W, Chen P, Jiang Y, et al. SIRT6 as a key event linking P53 and NRF2 counteracts APAP-induced hepatotoxicity through inhibiting oxidative stress and promoting hepatocyte proliferation. *Acta Pharm Sin B.* 2021;11(1):89–99. <https://doi.org/10.1016/j.apsb.2020.06.016>.

Publisher's Note

Springer Nature remains neutral with regard to jurisdictional claims in published maps and institutional affiliations.